Contrib Mineral Petrol (1986) 92:437–447

Contributions to Mineralogy and Petrology

Hydrothermal clinopyroxenes of the Skaergaard intrusion

Craig E. Manning and Dennis K. Bird
Department of Geology, Stanford University, Stanford, CA, 94305, USA

Abstract. Magmatic augites reacted with high temperature aqueous solutions to form secondary calcic pyroxenes during the subsolidus cooling of the Skaergaard intrusion. Secondary, hydrothermal clinopyroxenes replace wall rock igneous augites at the margins of veins filled with calcic amphibole. These veins are up to several millimeters wide and tens of meters in length. Hydrothermal clinopyroxenes are a ubiquitous and characteristic phase in the earliest veins throughout the Layered Series of the intrusion, and occur rarely in late veins that, in some places, crosscut the early veins. Associated secondary phases in early veins include amphiboles ranging in composition from actinolite to hornblende, together with biotite, Fe–Ti oxides and calcic plagioclase. Hydrothermal clinopyroxenes in late veins may be associated with actinolite, hornblende, biotite, magnetite and albite.

Hydrothermal clinopyroxenes are depleted in Fe, Mg and minor elements, and enriched in Ca and Si relative to igneous augites in the Layered Series gabbros. Secondary vein pyroxenes are similar in composition to calcic pyroxenes from amphibolite facies metamorphic rocks. Clinopyroxene solvus thermometry suggests minimum temperatures of equilibration of between 500° and 750° C. These temperatures, combined with numerical transport models of the intrusion, suggest that vein clinopyroxenes could have formed during 20,000 to 60,000 year time intervals associated with a maximum in the fluid flux through fractures in the Layered Series.

Introduction

The Skaergaard intrusion represents the uplifted and eroded roots of an Early Eocene hydrothermal system (Taylor and Forester 1979; Norton and Taylor 1979). Reactions between aqueous solutions in fractures (veins) and magmatic minerals began at high temperatures and continued throughout the cooling history of the intrusion, producing secondary, fracture-filling mineral assemblages that range from upper amphibolite to zeolite facies (Norton et al. 1984; Bird et al. 1986). Similar fracture-controlled hydrothermal alteration initiated at high temperatures has been recognized in synorogenic gabbros (e.g. Otten 1983, 1984), in oceanic dredge samples (e.g. Bonatti et al. 1975; Ito and Anderson 1983; Kimball and Spear 1983; Honnorez et al. 1984) and in many ophiolites (e.g. Liou and Ernst 1979; Stern and Elthon 1979; Evarts and Schiffman 1983).

An important index mineral associated with hydrothermal veins in the layered series of the Skaergaard intrusion is secondary, hydrothermal calcic clinopyroxene. These secondary clinopyroxenes are distinct in both texture and composition from exsolved magmatic calcic pyroxenes, which have been studied by Bown and Gay (1960), Nwe (1975, 1976), Nwe and Copely (1975), Coleman (1978), Nobugai et al. (1978), Nobugai and Morimoto (1979), and Nakajima and Hafner (1980). However, hydrothermal clinopyroxenes display compositional trends that correlate with stratigraphic elevation in the intrusion similar to the calcic pyroxene crystallization trend discussed by Wager and Deer (1939), Poldervaart and Hess (1951), Muir (1951), Brown (1957), Brown and Vincent (1963) and Lindsley et al. (1969). In this paper, the occurrence and compositional variation of secondary clinopyroxenes are described. Minimum temperature estimates of clinopyroxene formation based on solvus thermometry are combined with the transport models of the Skaergaard intrusion reported by Norton and Taylor (1979) to evaluate the temporal relationship between the formation of vein clinopyroxenes and hydrothermal fluid flux during the subsolidus cooling of the Layered Series gabbros.

Geologic setting

The 55 m.y. old Skaergaard intrusion was emplaced into the East Greenland continental margin during the early stages of opening of the North Atlantic ocean (Brooks and Gleadow 1977; Brooks and Nielsen 1982a, b). The present exposure of the Skaergaard magma chamber is oval in shape and extends about 10 kilometers north-south and 7 kilometers east-west (Fig. 1). That portion in contact with the host gneisses, basalts and sedimentary rocks constitutes the chilled Marginal Border Group. The main body of the magma crystallized from the bottom up to form the Layered Series and from the top down to form the Upper Border Group. These two crystallization sequences came together at the Sandwich Horizon. Fractional crystallization led to iron enrichment with increasing degree of crystallization in both the Layered Series and the Upper Border Group (Wager and Deer 1939; Wager and Brown 1967). The solidified gabbro fractured shortly after crystallization (Norton et al. 1984).

The intrusion has been depleted in ^{18}O to well below magmatic values by meteoric water circulating through the pluton at elevated temperatures (Taylor and Forester 1979). Numerical models of the heat and mass transfer associated with the crystallization and cooling of the Skaergaard intrusion have predicted temperatures,

Offprint requests to: C.E. Manning

volume averaged permeabilities and rates of fluid flux in the Skaergaard magma hydrothermal system (Norton and Taylor 1979). Norton and Taylor conclude that 75% of the fluid flux through the intrusion took place when average temperatures of the gabbro were greater than 480° C. Thus, these studies suggest that virtually all isotopic mass transfer occurred at high temperatures (>400–500° C).

Detailed mapping and mineralogic investigations of selected portions of the Layered Series have led to the identification of five hydrothermal vein types associated with the crystallization and cooling of the chamber (Bird et al. 1986). Alteration zones around some of these fractures show extreme ^{18}O depletions relative to the wall rock in which they occur (Taylor and Forester 1979), indicating that the fluids in the veins were responsible for the low $\delta^{18}O$ composition of the Skaergaard intrusion. The earliest set of hydrothermal veins found in the Layered Series are thin (1–2 mm wide; Fig. 2a) and continuous for tens of meters. These veins contain amphiboles ranging in composition from actinolite to hornblende, together with calcic clinopyroxenes, calcic plagioclase, biotite, ilmenite and magnetite (Bird and Rogers 1983; Bird and Manning 1984; Norton et al. 1984; Bird et al. 1986). In the Middle and Upper Zones, the earliest veins are commonly associated with, and in some places crosscut by, transgressive granophyres (Norton et al. 1984; Bird et al. 1986). These veins may form either parallel to granophyre-filled fractures or in complex splays and networks at granophyre fracture terminations (see Norton et al. 1984, Fig. 12). Other types of fractures are filled by the assemblages actinolitic hornblende – chlorite – talc – biotite; fayalite – cummingtonite – quartz – magnetite; hornblende – actinolite – biotite; and hornblende – actinolite – albite – epidote – prehnite (Bird et al. 1986). The latter two vein types contain rare hydrothermal clinopyroxenes, and, based on textures, mineral compositions and crosscutting relations discussed by Bird et al. (1986), are interpreted to have formed later than the early veins discussed above. Late veins are commonly associated with brecciation of the wall rock and display much wider alteration halos than the early vein set.

Occurrence

Secondary calcic pyroxenes form by replacement of magmatic augite[1] at the margins of veins filled by calcic amphiboles throughout the Layered Series gabbros (Fig. 1). They

1 The magmatic calcic pyroxenes of the Skaergaard intrusion, which include augites, ferroaugites and ferrohedenbergites, are referred to as augites for simplicity

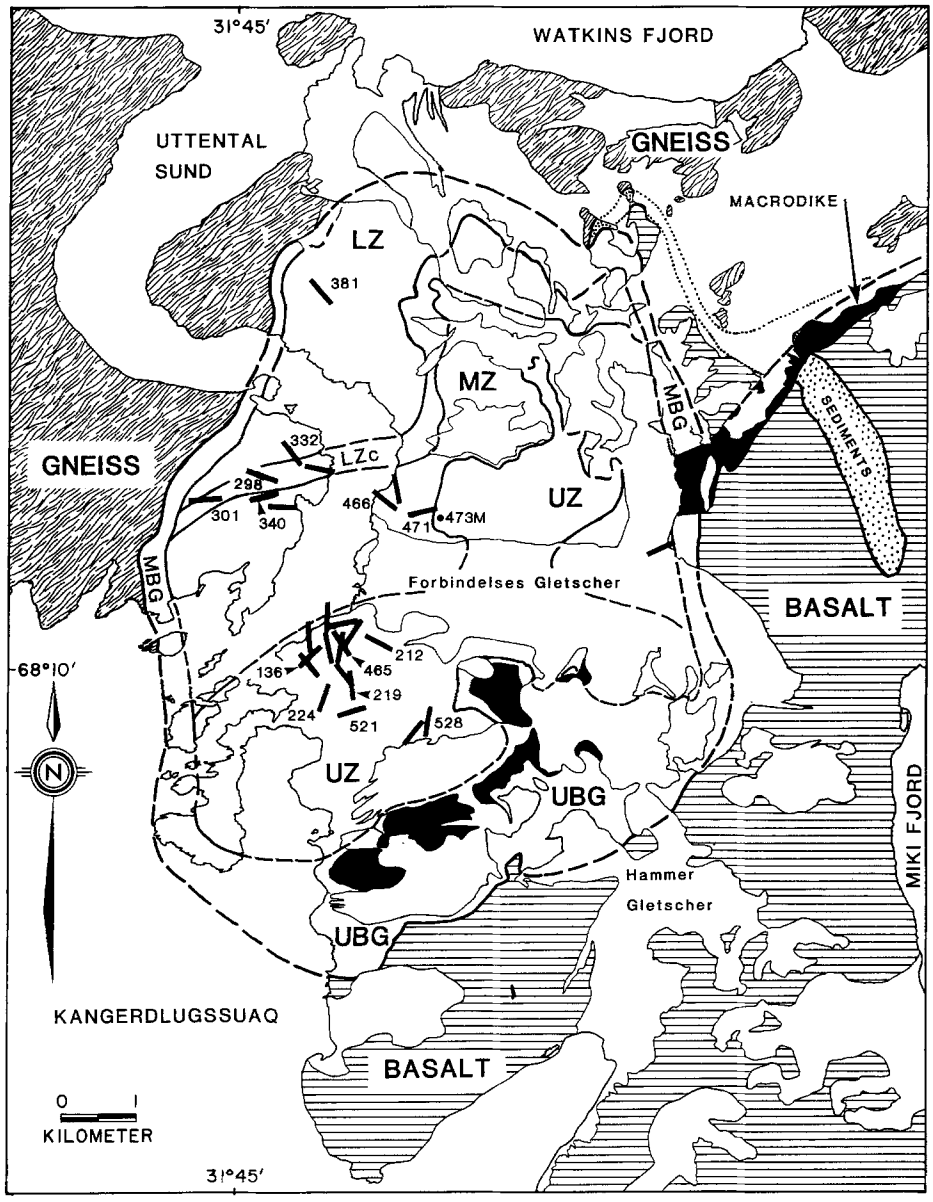

Fig. 1. Generalized geologic map of the Skaergaard intrusion showing distribution and orientation of hydrothermal pyroxene-bearing veins in the Layered Series. The size of bars denoting veins is not to scale. Numbers refer to samples discussed in text. MBG, LZ, MZ, UZ and UBG refer to the Marginal Border Group, the Lower, Middle and Upper Zones of the Layered Series and the Upper Border Group. The lack of sample locations in the northern portions of the intrusion is due to the rugged terrane which makes detailed fracture mapping and sampling difficult. The map is compiled from data reported by Wager and Deer (1939), Wager and Brown (1967), and A.R. McBirney (personal communication, 1983)

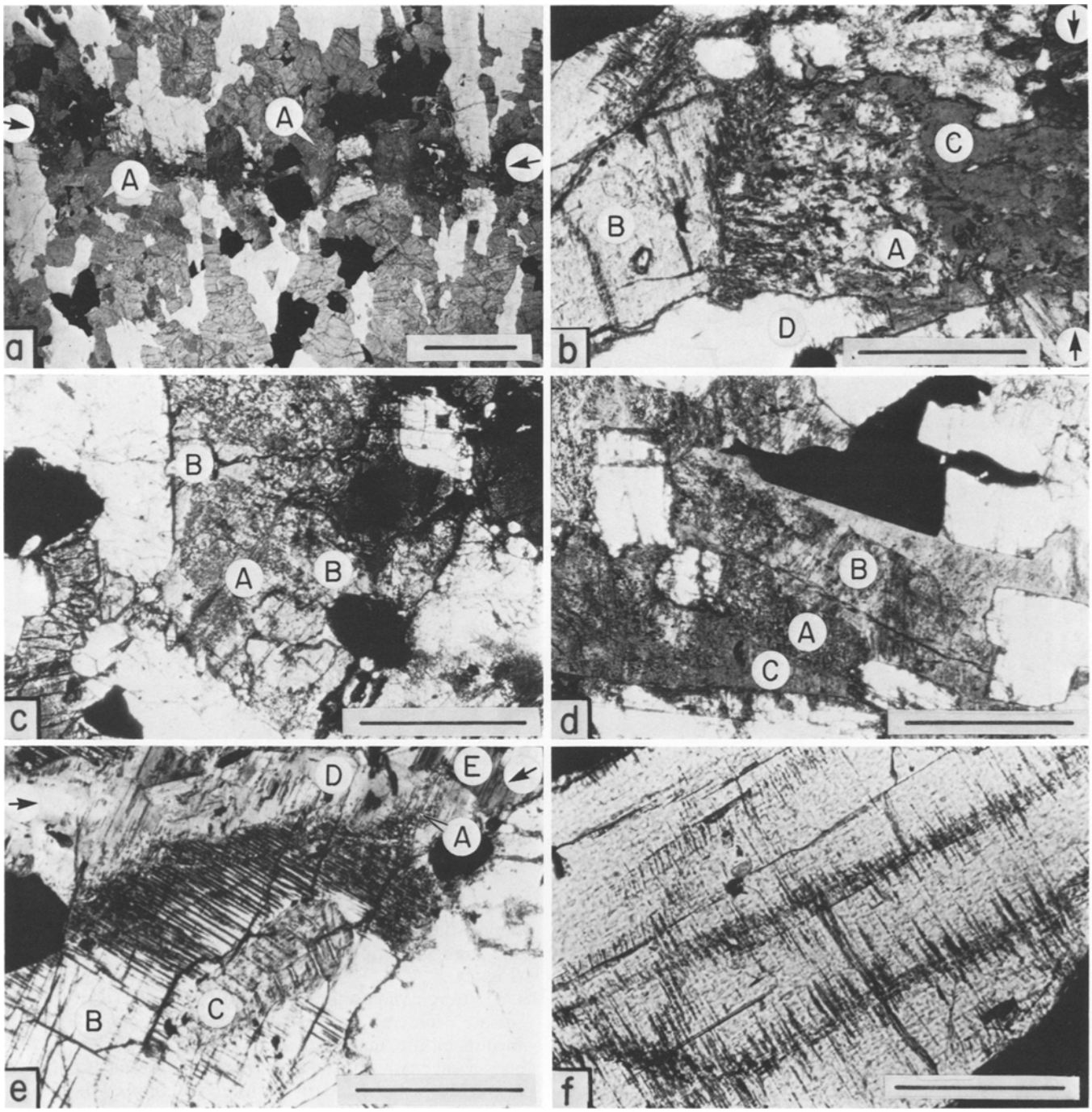

Fig. 2. **a** Plane light photomicrograph of early hydrothermal vein cutting Middle Zone gabbro (sample 471-EG82). *A* = secondary clinopyroxene replacing magmatic augites near vein margins. Vein position is marked by arrows. Scale bar is 3 mm. **b** Secondary clinopyroxene (*A*) replacing magmatic augite (*B*) at early vein margin (sample 466-EG82). Coexisting phases include vein filling amphibole (*C*), calcic plagioclase (*D*) and Fe–Ti oxides (small inclusions in secondary clinopyroxene). Vein is marked by arrows. Scale bar is 0.5 mm (plane light). **c** Plane light photomicrograph of green, secondary hedenbergite (*A*) replacing brown, magmatic ferrohedenbergite (*B*) several centimeters from an early vein in upper zone (528-EG82). Scale bar is 1 mm. **d** Plane light photomicrograph of secondary clinopyroxene (*A*) replacing magmatic augite (*B*) near a late vein (sample 301-EG82). Vein is filled by actinolite (*C*) and is out of the field of view to the left. Scale bar is 1 mm. **e** Plane light microphotograph showing dissolution of secondary clinopyroxene (*A*) in sample 332-EG82. Vein extends across top of photo. Magmatic augite (*B*) contains altered exsolution lamellae, and magmatic Ca-poor pyroxene (*C*) is completely replaced by actinolite. Early brown hornblende (*D*) is fractured and overgrown by late green hornblende (*E*). Scale bar is 1 mm. **f** Plane light photomicrograph showing exsolution coarsening and alteration along microfractures in magmatic augite (sample 298-EG82). Scale bar is 0.2 mm

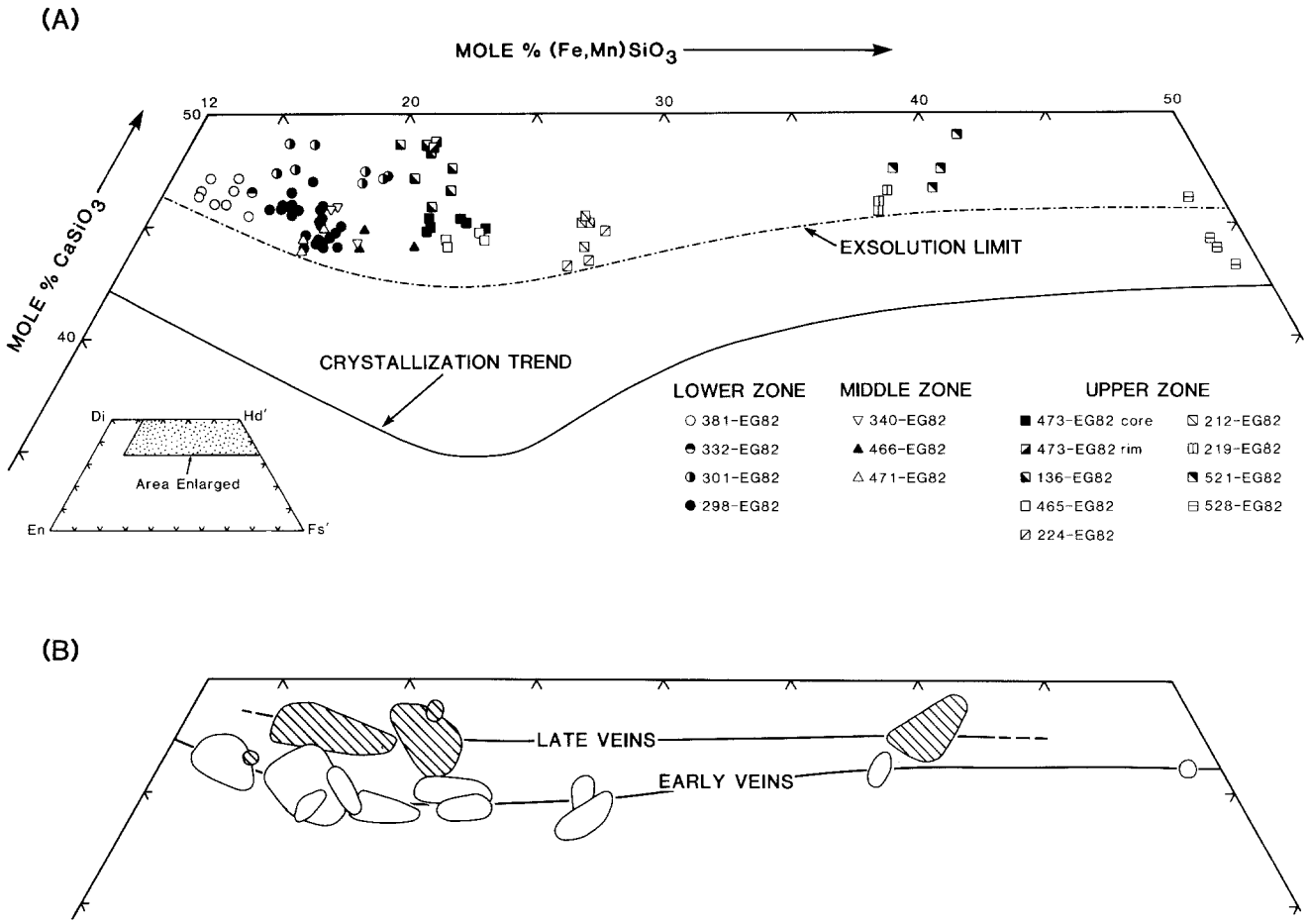

Fig. 3. **A** Plot of hydrothermal clinopyroxene analyses in the system $CaSiO_3-MgSiO_3-(Fe^{total},Mn)SiO_3$. *Inset* shows portion of the quadrilateral enlarged and position of pyroxene endmembers $Mg_2Si_2O_6$ (En), $CaMgSi_2O_6$(Di), $Ca(Fe^{total},Mn)Si_2O_6$(Hd′) and $(Fe^{total},Mn)_2Si_2O_6$(Fs′). Crystallization trend shown in *solid line* is after Brown (1957) and Brown and Vincent (1963). *Dash-dot line* denotes maximum Ca enrichment in magmatic augites due to exsolution (Nwe 1976). *Partially filled symbols* denote clinopyroxenes from late veins. **B** Pyroxene quadrilateral at the same scale as **A** showing the compositional distinction between pyroxenes from early veins (*no pattern*) and pyroxenes from late veins (*diagonally ruled pattern*). The field for 528-EG82 represents the rim composition of a zoned crystal (see text)

are colorless to light green, non-pleochroic, and usually form in optical continuity with the magmatic augites with which they are in contact. Hydrothermal clinopyroxenes have lower relief than magmatic augites and display no optically resolvable exsolution lamellae. These features clearly distinguish secondary pyroxenes from pink to brown, exsolved magmatic augites.

Early vein clinopyroxenes are blocky, anhedral crystals up to 0.5 mm in length and are intergrown with minute grains of magnetite, ilmenite and hornblende (Fig. 2b). All clinopyroxene-bearing early veins above the central portions of the Middle Zone are in close association with granophyres, whereas those below are not. Early vein clinopyroxenes associated with granophyres are commonly much larger than early vein clinopyroxenes from lower stratigraphic levels. In some areas of the Upper Zone, magmatic augites are replaced up to several centimeters from vein margins by green hydrothermal clinopyroxenes. Similar green hedenbergitic rims on ferrohedenbergites from the Sandwich Horizon have been interpreted by Brown and Vincent (1963), Lindsley et al. (1969, Fig. 3d) and Nwe and Copely (1975) as having crystallized from the most evolved Skaergaard magma. However, green clinopyroxenes that rim earlier pyroxenes from the Sandwich Horizon examined in this study have similar textures, compositions (see below) and optical properties as the hydrothermal pyroxenes (Fig. 2c).

Late veins containing secondary pyroxenes are rare. Associated minerals in these veins include actinolite, hornblende, biotite, magnetite and albite. Hydrothermal pyroxenes associated with late veins are fine grained, colorless aggregates with abundant inclusions of amphibole and oxides (Fig. 2d). These textures may represent retrograde reactions of pyroxenes formed at an earlier stage. Early veins which have been reopened and filled by late stage vein minerals including actinolite, hornblende and albite usually show textural evidence for reaction and dissolution of secondary pyroxenes (Fig. 2e).

In addition to the formation of clinopyroxenes at vein margins, magmatic augites display other evidence of reaction with hydrothermal fluids. Augites more than several centimeters from hydrothermal veins have (001) pigeonite lamellae that are <3 microns wide (Brown 1957; Bown and Gay 1960). Augites within 3 mm of some veins have (001) lamellae up to 6 microns wide. Taylor and Forester (1979) observed coarsened exsolution lamellae along microfractures in the Marginal Border Group and the Layered Series (see their plate 1B), and similar effects have been

observed in other layered gabbros (e.g. the Artfjället gabbro, Otten 1983). These features are common in wall rock augites in all samples examined during this investigation (Fig. 2f).

Coarsened lamellae of Ca-poor pyroxene in igneous augite are commonly altered to amphibole (e.g. Fig. 2e). Single crystal x-ray diffraction and transmission electron microscopic studies have identified clinoamphibole lamellae in samples from the Marginal Border Group (Smith 1977) and the Upper Border Group (Nakajima and Hafner 1980). Smith (1977) suggests that clinoamphibole formation was by exsolution, but considers the possibility of late stage alteration as well. Nakajima and Hafner (1980) conclude that clinoamphibole lamellae are alteration products. The common association of secondary clinoamphiboles within and near Skaergaard veins suggests that these clinoamphibole lamellae are formed by hydrolysis reactions with hydrothermal solutions rather than by exsolution.

Clinopyroxene compositions

Hydrothermal clinopyroxenes from representative samples and stratigraphic positions throughout the Layered Series were analyzed using a JEOL 733A automated electron microprobe with 5 wavelength dispersive spectrometers. Run conditions included an accelerating voltage of 15 Kv, 15 nA sample current on Faraday cup, 20 seconds maximum counting time and beam diameters of 1–3 microns. Standards were well characterized natural and synthetic silicate minerals. The Bence-Albee (1968) matrix correction method was employed.

Analyses of secondary clinopyroxenes from the Layered Series are shown on the pyroxene quadrilateral in Fig. 3a. Average analyses of hydrothermal clinopyroxenes from each sample shown in Fig. 3a are presented in Tables 1, 2 and 3. In the nomenclature of Poldervaart and Hess (1951), most hydrothermal clinopyroxenes range from salite to hedenbergite in composition. Several samples contain calcium-rich augites and ferroaugites as well. The calcic pyroxene crystallization trend defined by Brown (1957) and Brown and Vincent (1963), and the exsolution limit proposed by Nwe (1976) are also given in Fig. 3a for reference. Nwe's (1976) limit represents the maximum Ca-enrichment in host magmatic augites due to exsolution of a Ca-poor phase. Secondary clinopyroxenes associated with both early and late veins form a trend of increasing iron content with increasing stratigraphic elevation. Hydrothermal clinopyroxenes from all portions of the intrusion are more calcic than the most calcic augite produced by exsolution. Figure 3b illustrates that clinopyroxenes from late veins are more calcic than their early vein counterparts. Secondary clinopyroxenes from the early veins cluster along a line roughly 2% richer in the $CaSiO_3$ component than the observed $CaSiO_3$ limit in exsolved igneous augites. Pyroxenes from late veins are enriched in the $CaSiO_3$ component by about 4%.

Compositions of hydrothermal and magmatic calcic clinopyroxenes are shown in Fig. 4 as a function of stratigraphic height in the intrusion. It can be seen that hydrothermal clinopyroxenes are compositionally distinct from igneous augites in major elements. Hydrothermal clinopyroxenes from early veins are enriched in Ca relative to igneous augites with maximum enrichments in Upper Zone a. Secondary clinopyroxenes from late veins show even greater

Table 1. Hydrothermal clinopyroxenes from early veins

	381-EG82 (8)[c] 475 m[d]	298-EG82 (25) 775 m	340-EG82 (3) 875 m	466-EG82 (3) 1125 m
SiO_2	53.79	52.63	52.35	52.39
Al_2O_3	0.60	0.65	0.40	0.43
FeO[e]	8.79	10.89	11.84	12.57
Fe_2O_3[e]	0.02	0.47	0.17	0.83
MgO	13.94	12.81	12.25	12.12
MnO	0.26	0.23	0.19	0.35
TiO_2	0.11	0.11	0.10	0.08
Cr_2O_3	n.a.[f]	n.d.[g]	n.d.	0.01
CaO	22.83	22.07	21.96	21.78
Na_2O	0.15	0.14	0.13	0.12
Sum	100.49	100.00	99.39	100.68
Si[h]	1.995	1.983	1.991	1.978
Al^{IV}	0.005	0.017	0.009	0.019
Al^{VI}	0.021	0.011	0.009	0.000
Fe^{2+}	0.273	0.343	0.377	0.397
Fe^{3+}	0.001	0.013	0.005	0.024
Mg	0.770	0.719	0.694	0.682
Mn	0.008	0.007	0.006	0.011
Ti	0.003	0.003	0.003	0.002
Cr	0.000	0.000	0.000	0.000
Ca	0.907	0.891	0.895	0.881
Na	0.011	0.010	0.010	0.009
Sum	3.994	3.997	3.999	4.003

[a] Single analysis
[b] Reopened early vein
[c] Numbers in parentheses denote number of analyses used to obtain average
[d] Height in meters above lowermost exposure of Layered Series gabbro (see Wager and Brown, 1967, for stratigraphic column)
[e] FeO and Fe_2O_3 recalculated assuming charge balance (Papike et al., 1974)
[f] Not analyzed
[g] Not detected
[h] Cation proportions based on six oxygens

increases in Ca content relative to magmatic augite. Hydrothermal clinopyroxenes also contain more Si, though enrichments decrease with increasing stratigraphic elevation. Clinopyroxenes from late veins show slightly higher relative enrichments in Si, than those from early veins, though there is significant overlap of the two data sets. Ferrous iron and magnesium are both depleted in most hydrothermal clinopyroxenes, although Mg is slightly enriched in secondary clinopyroxenes relative to magmatic augites above Upper Zone b.

Igneous augites and hydrothermal clinopyroxenes are distinct in minor element composition as well (Fig. 5). Depletions in Al contents of secondary clinopyroxenes decrease with increasing elevation in the intrusion. Below Upper Zone a, clinopyroxenes from late veins show greater depletions than those in early veins, but above Upper Zone b, all secondary clinopyroxenes are virtually Al-free, and no compositional distinction is apparent. Magmatic augites show no systematic compositional trends in Ti concentrations, but Ti contents are lower in secondary pyroxenes of both types. Sodium contents of early vein clinopyroxenes decrease with increasing stratigraphic elevation to Upper

Table 2. Hydrothermal clinopyroxenes from early veins associated with granophyres

	471-EG82 (3) 1275 m	473m-EG82 core (6) 1580 m	465-EG82 (4) 1820 m	224-EG82 (3) 1950 m	212-EG82 (4) 2080 m	219-EG82 (3) 2250 m	528-EG82[a] rim 2480 m
SiO_2	52.58	51.62	52.12	50.90	52.21	49.50	48.55
Al_2O_3	0.57	0.32	0.30	0.19	0.26	0.13	0.18
FeO	11.34	14.10	14.76	17.46	17.16	22.86	28.93
Fe_2O_3	0.16	0.52	0.28	0.23	0.27	0.62	0.44
MgO	12.97	10.78	10.69	8.84	8.74	4.50	0.41
MnO	0.30	0.28	0.42	0.41	0.44	0.73	0.95
TiO_2	0.14	0.06	0.07	0.03	0.06	0.01	0.04
Cr_2O_3	n.a.	0.01	n.d.	n.d.	n.d.	n.d.	0.02
CaO	21.68	21.73	21.44	20.53	21.26	21.44	20.82
Na_2O	0.10	0.10	0.17	0.17	0.27	0.17	0.17
Sum	99.84	99.52	100.25	98.76	100.67	99.96	100.51
Si	1.985	1.986	1.992	2.000	2.007	1.986	1.994
Al^{IV}	0.015	0.014	0.008	0.000	0.000	0.006	0.006
Al^{VI}	0.010	0.001	0.006	0.008	0.012	0.000	0.003
Fe^{2+}	0.358	0.454	0.472	0.574	0.552	0.767	0.994
Fe^{3+}	0.005	0.015	0.008	0.007	0.008	0.019	0.014
Mg	0.730	0.618	0.609	0.518	0.501	0.269	0.025
Mn	0.010	0.009	0.014	0.014	0.014	0.025	0.033
Ti	0.004	0.002	0.002	0.001	0.002	0.000	0.001
Cr	0.000	0.000	0.000	0.000	0.000	0.000	0.001
Ca	0.877	0.896	0.878	0.864	0.876	0.922	0.916
Na	0.007	0.007	0.013	0.013	0.020	0.013	0.014
Sum	4.001	4.002	4.002	3.999	3.992	4.007	4.000

See Table 1 for footnotes

Table 3. Hydrothermal clinopyroxenes from late veins

	332-EG82[a, b] 720 m	301-EG82 (9) 750 m	473m-EG82[a] rim 1580 m	136-EG82 (7) 1720 m	521-EG82 (4) 2280 m
SiO_2	52.73	52.77	51.77	52.32	50.57
Al_2O_3	0.38	0.05	0.26	0.13	0.12
FeO	8.99	11.00	12.70	13.27	23.60
Fe_2O_3	0.69	0.18	0.52	0.23	0.05
MgO	13.54	12.05	10.39	10.69	3.59
MnO	0.18	0.26	0.27	0.31	1.04
TiO_2	0.08	0.04	0.04	0.04	0.01
Cr_2O_3	n.a.	n.d.	0.04	n.d.	0.01
CaO	22.96	23.29	23.59	23.31	22.08
Na_2O	0.10	0.09	0.09	0.07	0.09
Sum	99.65	99.73	99.67	100.37	101.16
Si	1.983	2.000	1.986	1.993	2.007
Al^{IV}	0.017	0.000	0.012	0.006	0.000
Al^{VI}	0.000	0.002	0.000	0.000	0.006
Fe^{2+}	0.283	0.349	0.408	0.423	0.783
Fe^{3+}	0.020	0.005	0.015	0.007	0.001
Mg	0.759	0.681	0.594	0.607	0.212
Mn	0.006	0.008	0.009	0.010	0.035
Ti	0.002	0.001	0.001	0.001	0.000
Cr	0.000	0.000	0.001	0.000	0.000
Ca	0.925	0.946	0.970	0.951	0.939
Na	0.007	0.007	0.007	0.005	0.007
Sum	4.002	3.999	4.003	4.003	3.990

See Table 1 for footnotes

Zone a, then increase above this, and late vein clinopyroxenes from all parts of the Layered Series are more depleted in Na than those from early veins. Manganese contents of secondary clinopyroxenes are similar to those of magmatic augites from the Lower Zone to Upper Zone b, but Mn is enriched in secondary clinopyroxenes in the Upper parts of Upper Zone b and higher. Chromium (not shown in Fig. 4) was not detected in most magmatic and hydrothermal clinopyroxenes. Calculated Fe^{3+} contents vary widely but are not considered accurate because of the dependence of such calculations on the quality of the analyses of other constituent elements, especially Si (e.g. Robinson 1980; Lindsley and Anderson 1983).

Data from vein 528-EG82 (Fig. 3a) represent compositional zoning across a green hedenbergite rim on a brown magmatic ferrohedenbergite near the Sandwich Horizon. The least calcic analysis is of green hedenbergite in contact with brown ferrohedenbergite, and the most calcic analysis is of green hedenbergite in contact with vein amphibole. Nwe and Copley (1975) present an analysis of a green hedenbergite rim from near the Sandwich Horizon (see their Table 1, analysis 8) similar in composition to the hedenbergite in 528-EG82 (Table 2). This coupled with the textural evidence discussed above, suggest that these rims represent secondary clinopyroxenes.

Comparison to other hydrothermal and metamorphic clinopyroxenes

Calcic pyroxenes form in a variety of hydrothermal and metamorphic environments. Augitic and salitic pyroxenes form in the highest temperature zones of active geothermal

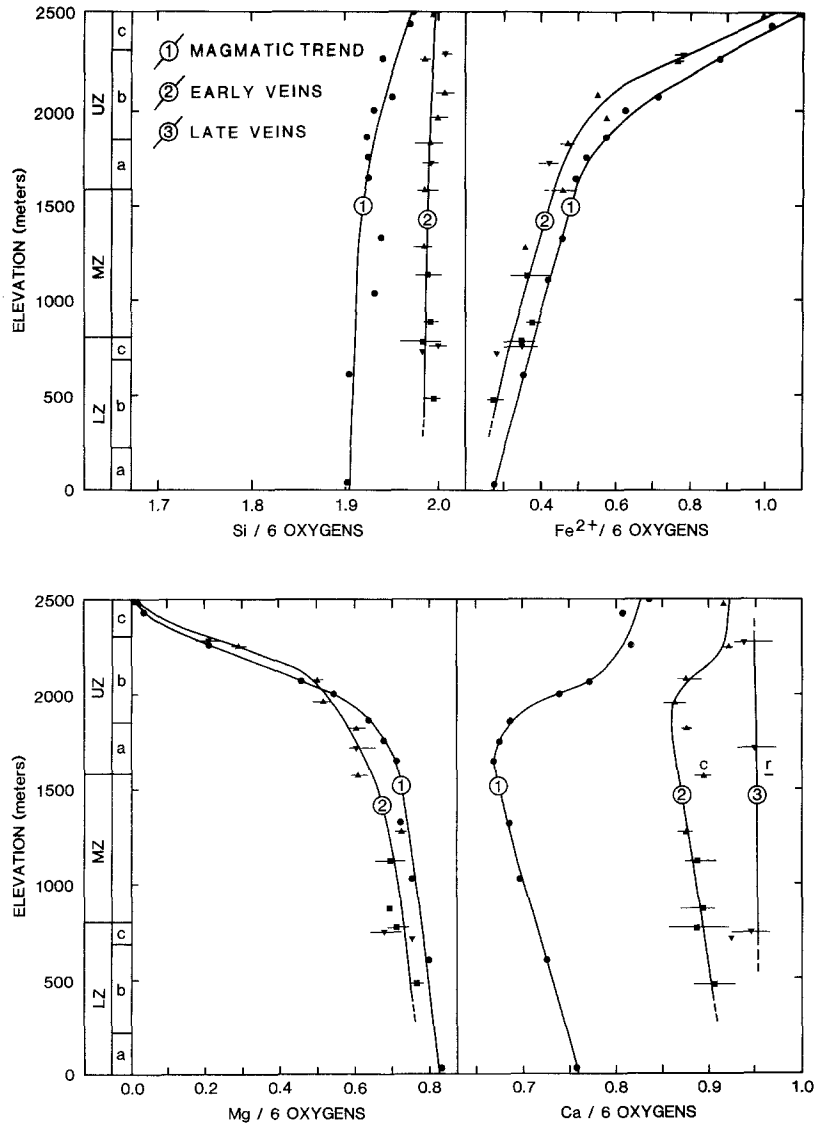

Fig. 4. Cation proportions of Si, Fe^{2+}, Mg and Ca per six oxygens vs. stratigraphic position for hydrothermal clinopyroxenes and magmatic augites (see Fig. 1 for sample locations). *Circles* represent the magmatic augite data of Brown (1957) and Brown and Vincent (1963), *squares* represent hydrothermal clinopyroxenes from early veins, *triangles* represent hydrothermal clinopyroxenes from veins associated with granophyres, and *inverted triangles* indicate secondary clinopyroxenes from late veins. *Symbols* represent average analyses of hydrothermal clinopyroxenes presented in Tables 1, 2 and 3, and the bars denote the range in analyses. Approximate compositional trends are shown for magmatic augites (*curve 1*) and early vein clinopyroxenes (*curve 2*). Compositional trends of late vein clinopyroxenes (*curve 3*) are shown where distinct from early vein clinopyroxenes. Core (*c*) and rim (*r*) compositions of a zoned grain in 473m-EG82 are indicated where distinct

systems (Bird et al. 1984) and in the early metamorphic or main stage metasomatic stage of skarn formation (e.g. Einaudi et al. 1981). In regional metamorphic environments, calcic pyroxenes begin to form in metabasites in the middle to upper amphibolite facies (e.g. Spear 1981). Average compositions of hydrothermal clinopyroxenes from the Skaergaard intrusion are given in Fig. 6, together with selected calcic pyroxenes from these three environments. It can be seen that Skaergaard hydrothermal clinopyroxenes have Ca contents consistently lower than those from both active geothermal systems and skarn environments, but overlap completely with augites and salites from regional metamorphic rocks. The minor element contents of hydrothermal clinopyroxenes from the Skaergaard intrusion are lower than those of clinopyroxenes from all three environments.

Discussion

Clinopyroxene compositions can be used to estimate the minimum temperatures of vein formation (Lindsley and Anderson 1983; Lindsley 1983). Figure 7 shows compositions of secondary pyroxenes from the Skaergaard intrusion with the one atmosphere solvus. Use of the 1 atmosphere solvus diagram rather than the 5 kilobar diagram is based on the work of Lindsley et al. (1969), McBirney (1975) and reconstructions of the regional stratigraphy (e.g. Nielsen et al. 1981, and references therein), which suggest that pressures were about one kilobar or lower in the Layered Series. Figure 7 indicates that there is a decrease in the minimum temperature of clinopyroxene equilibration with increasing stratigraphic height. Minimum temperatures of clinopyroxenes from the early veins from the Lower Zone and Middle Zone are between 500° and about 750° C. Minimum temperatures of early vein pyroxenes in the Upper Zone below the middle of Upper Zone b range from 500° to 600° C, and those from central Upper Zone b and higher are less than 500° C. Pyroxenes from late veins all yield minimum temperatures below 500° C. Minimum temperatures estimated using equations reported by Kretz (1982) are greater by 50° to 100° C, perhaps because the metamorphic pyroxenes used to calibrate the lower temperature isotherms (e.g. the Quarading suite of Davidson 1968) are richer in minor components, particularly aluminum.

Temperatures of 500° to about 750° C correspond to amphibolite facies metamorphic conditions. Spear (1981)

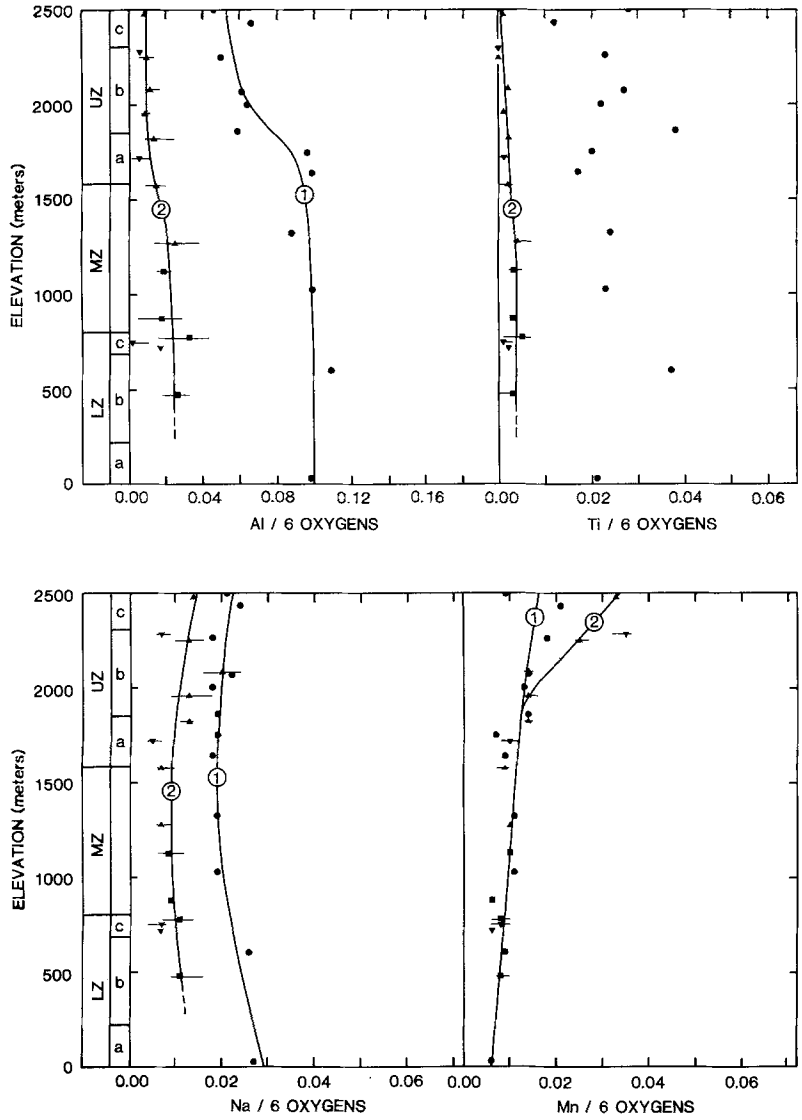

Fig. 5. Cation proportions of Al, Ti, Na and Mn per six oxygens vs. stratigraphic position for hydrothermal clinopyroxenes and magmatic augites (see Fig. 1 for sample locations). *Circles* represent the magmatic augite data of Brown (1957) and Brown and Vincent (1963), *squares* represent hydrothermal clinopyroxenes from early veins, *triangles* represent hydrothermal clinopyroxenes from veins associated with granophyres, and inverted triangles indicate secondary clinopyroxenes from late veins. *Symbols* represent average analyses of hydrothermal clinopyroxenes presented in Tables 1, 2 and 3, and the bars denote the range in analyses. *Lines* represent approximate compositional trends of magmatic augites (*1*) and early vein clinopyroxenes (*2*)

has shown that in rocks of olivine tholeiite composition, augite begins to form at approximately 740° C at one kilobar fluid pressure on the quartz-fayalite-magnetite oxygen buffer. These conditions correspond to pressures and oxygen fugacities inferred for the early veins in the Skaergaard magma hydrothermal system (Bird et al. 1986). Most minimum temperature estimates of Skaergaard vein pyroxenes are lower than this.

Constraints on minimum temperature of vein formation can be combined with the numerical models of Norton and Taylor (1979) to evaluate conditions and timing of formation of hydrothermal clinopyroxenes. The predicted time and volume averaged permeability of the Skaergaard intrusion which best fits observed ^{18}O depletions is 10^{-13} cm^2. Field and mineralogic relations reported by Norton et al. (1984) indicate that permeability decreased through time as high temperature fractures sealed with hydrothermal minerals, and that the permeability of the gabbros was $>10^{-13}$ while high temperature minerals were forming. The variation of the fluid flux with temperature reported by Norton and Taylor (1979) for a time and volume averaged permeability of 10^{-12} cm^2 of the intrusion is shown in Fig. 8 for two points in the Middle Zone. These two points are roughly equivalent to the positions of vein samples 340-EG82 (curve a), near the outer margins of the intrusion, and 466-EG82 (curve b), in the middle of the intrusion (see Fig. 1 for locations).

The highest minimum temperatures of equilibration of hydrothermal clinopyroxenes in early veins are about 750° C. For the outer areas of Middle Zone, these temperatures correspond to the large increase in mass flux at about 150,000 years in Norton and Taylor's model. In the central Middle Zone, 750° C is not attained until about 60,000–70,000 years later. The fact that solvus thermometry yields only a minimum temperature estimate coupled with the likelihood of reequilibration of early formed vein pyroxenes suggests that temperatures of formation of early vein pyroxenes could have been higher. This is consistent with the prediction that there was significant flux of fluids through fractures at temperatures greater than 750° C (Norton and Taylor 1979; Norton et al. 1984).

Below 750° C, temperatures drop rapidly as fluid flux increases. The 500° C minimum temperature estimate for early vein clinopyroxenes corresponds to the mass flux maximum for the central Middle Zone. Near the margins of the Middle Zone, mass flux continues to increase to a maxi-

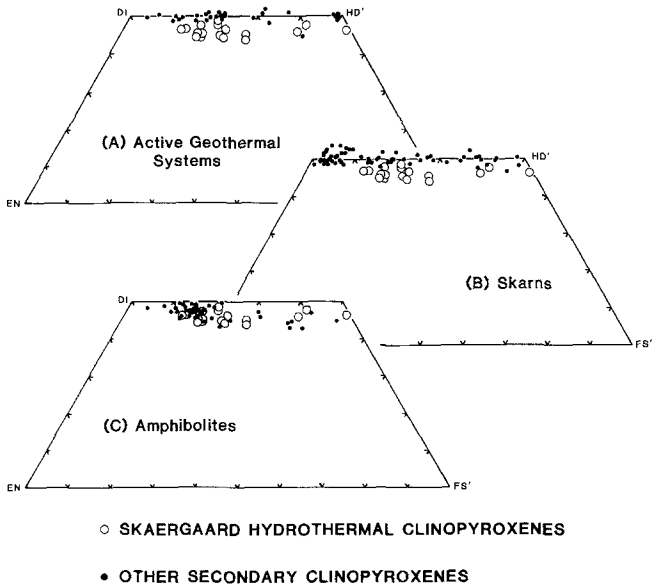

Fig. 6A–C. Pyroxene quadrilaterals showing secondary calcic pyroxenes from the Skaergaard intrusion (*open circles*) and calcic pyroxenes (*dots*) from: **A** active geothermal systems (Cavaretta et al. 1982; Bird et al. 1984; Schiffman et al. 1985), **B** representative skarn environments (tungsten skarns: Newberry 1980; porphyry copper-related skarns: Harris 1979; Meinert 1980; and lead-zinc skarns: Yun and Einaudi 1982), and **C** calcic clinopyroxene-bearing amphibolites (Miyashiro 1958; Shido 1958; Binns 1965; Ghent et al. 1975; Floran and Papike 1978; Kretz 1978; Ghent and Stout 1981; Jamieson 1981; Liou et al. 1981; Hill 1984; Honnorez et al. 1984). Abbreviations for quadrilateral endmembers are the same as in Fig. 3

mum at 300° C. The minimum temperatures of equilibration of hydrothermal clinopyroxenes correspond to times of rapid temperature decreases as fluid flux increased to maximum values in the fractured Layered Series gabbros. Fracture sealing by early vein minerals would cause a decrease in mass fluid flux at temperatures higher than those shown in Fig. 8. The fact that early veins commonly do not contain low temperature vein minerals such as coexisting actinolite and hornblende, albite, epidote and prehnite that occur in late veins is strong evidence in support of fracture sealing. Thus, it seems likely that many early fractures sealed at the time of or shortly after secondary clinopyroxene equilibration, and therefore that this equilibration corresponded to periods of the greatest mass flux of H_2O in early veins. The lack of fracture sealing, resulting in large fluid flux at lower temperatures in the outer margins of the intrusion, may explain late vein clinopyroxenes such as those of 301-EG82 (see Fig. 1). However, there is no systematic regional distribution of the clinopyroxene-bearing late veins.

Figure 8 also shows that temperatures of early vein pyroxene equilibration were maintained in the outer part of the Middle Zone for only about 20,000 years and in the central Middle Zone for about 60,000 years. These time intervals represent maximum times of pyroxene of formation.

Conclusions

Hydrothermal fluids in veins reacted with magmatic augites in the Skaergaard intrusion to form secondary clinopyroxenes ranging in composition from salite to hedenbergite with minor augite and ferroaugite. These pyroxenes form at vein margins between magmatic augites and vein filling amphibole. Secondary clinopyroxenes from early veins are texturally and compositionally distinct from those associated with late veins. In addition, hydrothermal clinopyroxenes from both vein types are texturally and compositionally distinct from magmatic augites. The most diagnostic compositional feature is the enrichment relative to magmatic augites of one to three mole percent $CaSiO_3$ component in early vein pyroxenes and $CaSiO_3$ enrichments of usually more than three mole percent in late vein clinopyroxenes. Other compositional characteristics include depletions in minor elements, Si enrichments, and widely variable

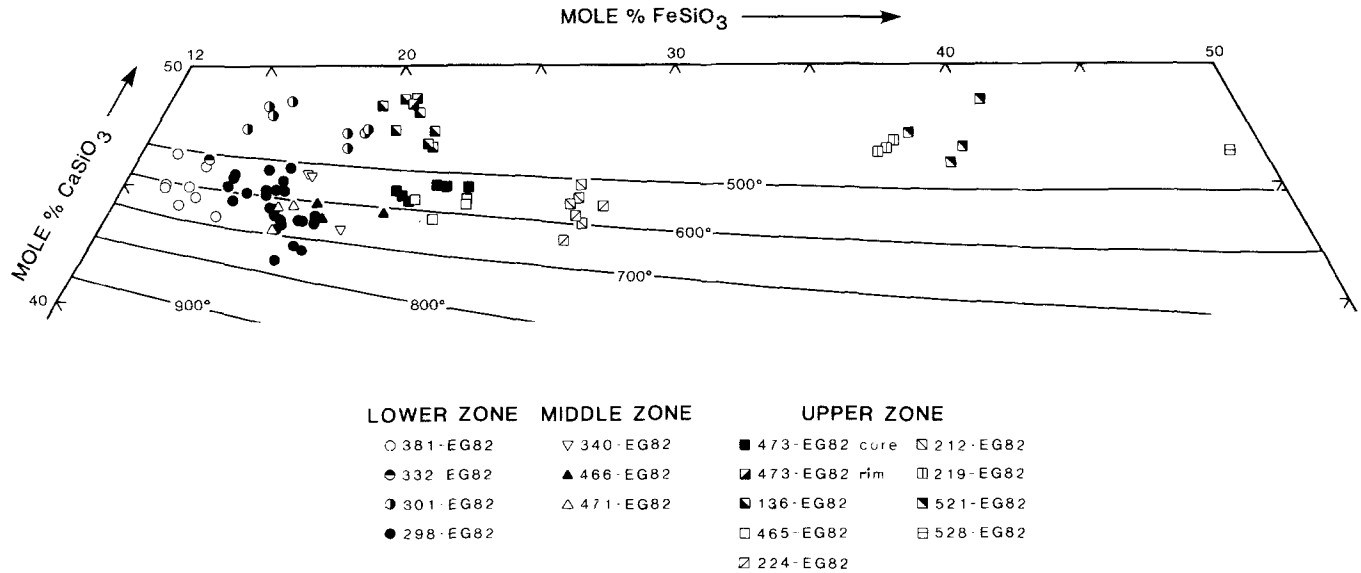

Fig. 7. Hydrothermal pyroxene compositions plotted on the pyroxene quadrilateral with the 1 atmosphere pyroxene solvus (Lindsley and Anderson 1983; Lindsley 1983). Clinopyroxene analyses were recalculated using equations presented by Lindsley and Anderson (1983)

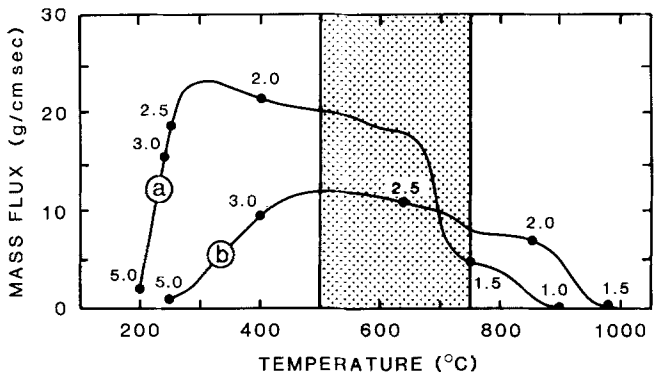

Fig. 8. Calculated mass fluid flux vs. temperature for two points corresponding approximately to the positions of 340-EG82 (a) and 466-EG82 (b). Data are taken from Norton and Taylor (1979) (see text). Filled circles denote years ($\times 10^6$) after the emplacement of the Skaergaard magma. The stippled region represents the minimum temperature range of early vein clinopyroxene equilibration

Fe/Mg ratios. These compositional features are produced by reactions between magmatic augites and hydrothermal fluids in vein systems during the subsolidus cooling history of the Skaergaard intrusion.

Hydrothermal clinopyroxenes from the Skaergaard intrusion resemble amphibolite facies metamorphic pyroxenes more than geothermal or skarn pyroxenes. Minimum temperatures of equilibration of early vein clinopyroxenes derived by solvus thermometry decrease with increasing stratigraphic height in the intrusion. These temperature estimates are 500° C to about 750° C in the Lower and Middle Zones, 500° C to 600° C in the lower portions of the Upper Zone, and below 500° C near the Sandwich Horizon. Late vein clinopyroxenes yield minimum temperature estimates of less than 500° C. Temperatures estimated for early vein clinopyroxenes throughout most of the intrusion correspond to middle to upper amphibolite facies metamorphic conditions at low pressures. Secondary clinopyroxene compositions corroborate previous predictions of a high temperature hydrothermal system at the Skaergaard intrusion (Taylor and Forester 1979; Norton and Taylor 1979). Comparison of pyroxene equilibration temperatures to the transport models of the Skaergaard intrusion of Norton and Taylor (1979) indicates that the vein clinopyroxenes were stable for relatively short time periods (20,000–60,000 years) during maxima in the fluid flux in fractures.

Acknowledgements. This paper has been substantially improved by the critical comments of John Ferry and William Carlson. We are indebted to Bob Coleman, Marco Einaudi, Minik Rosing, Moonsup Cho and Nick Rose for helpful reviews of early drafts of the manuscript. Thanks are also due Don Lindsley for comments on pyroxene analyses and Peter Schiffman for generously supplying unpublished data. Various aspects of the field and laboratory research have benefitted from our association with Kent Brooks, Troels Nielsen, T. Hauge Anderson, Alexander McBirney, Hugh Taylor, Denis Norton, T.N. Irvine, Minik Rosing, Nick Rose, Bobbie Bishop, Halldora Hregvidsdottir and Chuck Karish. The support of the National Science Foundation (NSF-EAR 82-15120 and NSF-EAR 84-18129) is gratefully acknowledged.

References

Bence AE, Albee AL (1968) Empirical correction factors for the electron microanalysis of silicates and oxides. J Geol 76:382–403

Binns RA (1965) The mineralogy of metamorphosed basic rocks from the Willyama complex, Broken Hill district, New South Wales. Part II. Pyroxenes, garnets, plagioclases, and opaque oxides. Mineral Mag 35:561–587

Bird DK, Rogers RD (1983) Fracture controlled hydrothermal alterations of the Skaergaard intrusion, Kangerdlugssuaq, East Greenland. Geol Soc Am Abstr with Programs 15:526

Bird DK, Manning CE (1984) Mineralogic record of hydrothermal fluid flow in the layered series of the Skaergaard intrusion. Geol Soc Am Abstr with Programs 16:445

Bird DK, Schiffman P, Elders WA, Williams AE, McDowell SD (1984) Calc-silicate mineralization in active geothermal systems. Econ Geol 79:671–695

Bird DK, Rogers RD, Manning CE (1986) Mineralized fracture systems of the Skaergaard intrusion. Meddr Grønland, Geoscience (in press)

Bonatti E, Honnorez J, Kirst P, Radicati F (1975) Metagabbros from the Mid-Atlantic ridge at 06°N: contact-hydrothermal-dynamic metamorphism beneath the axial valley. J Geol 83:61–78

Bown MG, Gay P (1960) An X-ray study of exsolution phenomena in the Skaergaard pyroxenes. Mineral Mag 32:379–388

Brooks CK, Gleadow AJW (1977) A fission-track age for the Skaergaard intrusion and the age of the East Greenland basalts. Geology 5:539–540

Brooks CK, Nielsen TFD (1982a) The E Greenland continental margin: a transition between oceanic and continental magmatism. J Geol Soc London 139:265–275

Brooks CK, Nielsen TFD (1982b) The Phanerozoic development of the Kangerdlugssuak area, East Greenland. Meddr Grønland, Geoscience 6:30 pp

Brown GM (1957) Pyroxenes from the early and middle stages of fractionation of the Skaergaard intrusion, East Greenland. Mineral Mag 31:511–543

Brown GM, Vincent EA (1963) Pyroxenes from the late stages of fractionation of the Skaergaard intrusion. J Petrol 4:175–197

Cavaretta G, Gianelli G, Puxeddu M (1982) Formation of authigenic minerals and their use as indicators of the physicochemical parameters of the fluid in the Larderello-Travale geothermal field. Econ Geol 77:1071–1084

Coleman LC (1978) Solidus and subsolidus compositional relationships of some coexisting Skaergaard pyroxenes. Contrib Mineral Petrol 66:221–227

Davidson LR (1968) Variations in ferrous iron-magnesium distribution coefficients of metamorphic pyroxenes from Quairading, Western Australia. Contrib Mineral Petrol 19:239–259

Einaudi MT, Meinert LD, Newberry RJ (1981) Skarn deposits. Econ Geol 75th Anniv Vol:317–391

Evarts RC, Schiffman P (1983) Submarine hydrothermal metamorphism of the Del Puerto ophiolite, California. Am J Sci 283:289–340

Floran RJ, Papike JJ (1978) Mineralogy and petrology of the Gunflint Iron Formation, Minnesota-Ontario: correlation of compositional and assemblage variations at low to moderate grade. J Petrol 19:215–288

Ghent ED, Nicholls J, Stout MZ, Rottenfusser B (1975) Clinopyroxene amphibolite boudins from Three Valley Gap, British Columbia. Can Mineral 15:269–282

Ghent ED, Stout MZ (1981) Metamorphism at the base of the Samail ophiolite, southeastern Oman Mountains. J Geophys Res 86:2557–2571

Harris NB (1979) Skarn formation near Ludwig, Yerington district, Nevada. Stanford University unpub PhD thesis.

Hill LB (1984) A tectonic and metamorphic history of the north-central Klamath Mountains, California. Stanford University, unpub PhD thesis

Honnorez J, Mével C, Montigny R (1984) Geotectonic significance of gneissic amphibolites from the Vema fracture zone, equitorial Mid-Atlantic ridge. J Geophys Res 89:11,379–11,400

Ito E, Anderson AT (1983) Submarine metamorphism of gabbros from the Mid-Cayman rise: petrographic and mineralogic con-

straints on hydrothermal processes at slow spreading ridges. Contrib Mineral Petrol 82:371–388
Jamieson RA (1981) Metamorphism during ophiolite emplacement – the petrology of the St. Anthony Complex. J Petrol 22:397–449
Kimball KL, Spear FS (1983) High temperature alteration sequence for abyssal ultramafics. Geol Soc Am Abstr with Programs 15:613
Kretz R (1978) Distribution of Mg, Fe^{2+}, and Mn in some calcic pyroxene – hornblende – biotite – garnet gneisses and amphibolites from the Grenville province. J Geol 86:599–619
Kretz R (1982) Transfer and exchange equilibria in a portion of the pyroxene quadrilateral as deduced from natural and experimental data. Geochim Cosmochim Acta 46:411–421
Lindsley DH (1983) Pyroxene thermometry. Am Mineral 68:477–493
Lindsley DH, Brown GM, Muir ID (1969) Conditions of the ferrowollastonite-ferrohedenbergite inversion in the Skaergaard intrusion, East Greenland. Min Soc Am Spec Pap 2:193–201
Lindsley DH, Anderson DJ (1983) A two pyroxene thermometer. J Geophys Res 88 (suppl):A887–A906
Liou JG, Ernst WG (1979) Oceanic rigde metamorphism of the East Taiwan ophiolite. Contrib Mineral Petrol 68:335–348
Liou JG, Ernst WG, Moore DE (1981) Geology and petrology of some polymetaorphosed amphibolites and associated rocks in northeastern Taiwan: Summary. Geol Soc Am Bull 92:219–224
McBirney AR (1975) Differentiation of the Skaergaard intrusion. Nature 253:691–694
Meinert LD (1980) Skarn, manto and breccia pipe formation in sedimentary rocks in the Cananea district, Sonora, Mexico. Stanford University unpub PhD thesis, pp 232
Miyashiro A (1958) Regional metamorphism of the Gosaisyo – Takanuki district in the central Abakuma plateau. Tokyo University J Fac Sci 11:219–278
Muir ID (1951) The clinopyroxenes of the Skaergaard intrusion, eastern Greenland: Mineral Mag 29:690–714
Nakajima Y, Hafner SS (1980) Exsolution in augite from the Skaergaard intrusion. Contrib Mineral Petrol 72:101–110
Newberry RJ (1980) The geology and chemistry of skarn formation and tungsten deposition in the central Sierra Nevada, California. Stanford University unpub PhD thesis
Nielsen TFD, Soper NJ, Brooks CK, Faller AM, Higgins AC, Matthews DW (1981) The pre-basaltic sediments and the lower basalts at Kangerdlugssuak, East Greenland. Meddr Grønland, Geoscience 6:28 pp
Nobugai K, Tokonami M, Morimoto N (1978) A study of subsolidus relations of the Skaergaard pyroxenes by analytical electron microscopy. Contrib Mineral Petrol 67:111–117
Nobugai K, Morimoto N (1979) Formation of pigeonite lamellae in Skaergaard augite. Phys Chem Mineral 4:361–371
Norton D, Taylor HP (1979) Quantitative simulation of the hydrothermal systems of crystallizing magmas on the basis of transport theory and oxygen isotope data: an analysis of the Skaergaard intrusion. J Petrol 20:421–486
Norton D, Taylor HP, Bird DK (1984) The geometry and high temperature brittle deformation of the Skaergaard intrusion. J Geophys Res 89:10,178–10,192
Nwe YY (1975) Two different pyroxene crystallization trends in the trough bands of the Skaergaard intrusion, East Greenland. Contrib Mineral Petrol 49:285–300
Nwe YY (1976) Electron probe studies of the earlier pyroxenes and olivines from the Skaergaard intrusion, East Greenland. Contrib Mineral Petrol 55:105–126
Nwe YY, Copely PA (1975) Chemistry, subsolidus relations and electron petrography of pyroxenes from the late ferrodiorites of the Skaergaard intrusion, East Greenland. Contrib Mineral Petrol 53:37–54
Otten MT (1983) The magmatic and subsolidus evolution of the Artfjället gabbro, central Swedish Caledonides. University of Utrecht (Netherlands), unpub PhD thesis
Otten MT (1984) The origin of brown hornblende in the Artfjället gabbro and dolerites. Contrib Mineral Petrol 86:189–199
Papike JJ, Cameron KL, Baldwin K (1974) Amphiboles and clinopyroxenes: Characterization of OTHER than quadrilateral components and estimates of ferric iron from microprobe data. Geol Soc Am Abstr with Programs 6:1053–1054
Poldervaart A, Hess HH (1951) Pyroxenes in the crystallization of basaltic magma. J Geol 59:472–489
Robinson P (1980) the composition space of terrestrial pyroxenes – internal and external limits. In: Prewitt CT (ed) Pyroxenes. Min Soc Am Rev Mineral 7:419–494
Schiffman P, Bird DK, Elders WA (1985) Hydrothermal mineralogy of calcareous sandstones from the Colorado River delta in the Cerro Prieto geothermal system, Baja California, Mexico. Mineral Mag 49:435–449
Shido F (1958) Plutonic and metamorphic rocks of the Nakoso and Iritono districts in the central Abakuma plateau. Tokyo University J Fac Sci 11:131–217
Smith PPK (1977) An electron microscopic study of amphibole exsolution in augites. Contrib Mineral Petrol 59:317–322
Spear FS (1981) An experimental study of hornblende stability and compositional variability in amphibolite. Am J Sci 281:697–734
Stern C, Elthon D (1979) Vertical variations in the effects of hydrothermal metamorphism in Chilean ophiolites: their implications for ocean floor metamorphism. Tectonophysics 55:179–213
Taylor HP, Forester RW (1979) An oxygen isotope study of the Skaergaard intrusion and its country rocks: a description of a 55-m.y. old fossil hydrothermal system. J Petrol 20:355–419
Wager LR, Brown GM (1967) Layered Igneous Rocks. WH Freeman, San Francisco, 588 pp
Wager LR, Deer WA (1939) Geological investigations in East Greenland, Part 3. The petrology of the Skaergaard intrusion, Kangerdlugssuak region. Meddr Grønland 105:352 pp
Yun S, Einaudi MT (1982) Zinc-lead skarns of the Yeonhwa-Ulchin district, South Korea. Econ Geol 77:1013–1032

Accepted November 5, 1985